Reducing steam transport pipe temperatures in power plants

Christopher Wales[a], Michael Tierney[a], Martyn Pavier[a], Peter EJ Flewitt[b]

[a]*Department of Mechanical Engineering, University of Bristol, Bristol, UK*
[b]*School of Physics, University of Bristol, Bristol, UK*

Abstract

A cycle analysis has been applied to a model of a advanced ultra-supercritical steam plant with novel steam pipes. The transfer pipes proposed incorporate internal thermal coatings and are externally jacketed to enable cooling. This enables higher temperature working steam, while keeping the pipe wall temperature below the acceptable limit for more conventional steel alloys and avoiding the need to use higher cost austenitic stainless steels and nickel base alloys. The baseline design had a superheat temperature of 700 °C and a reheat temperature of 720 °C. A thermal coating thickness of 2.8 mm is sufficient to keep the wall temperatures of the steam transfer pipe after the supercritical boiler below 600 °C. For the transfer pipe located after the reheater a thicker coating or less ambitious reheat temperature is required to achieve acceptable pipe wall temperatures. Whereas subcritical plant has a calculated cycle efficiency of 42.1%, the elevated temperature and pressure in a customary ultra-supercritical steam boost cycle efficiency to 52.2%. Modifying this design with a thermal barrier lowers the cycle efficiency to 51.4%, still appreciably better than for subcritical plant. Alternative plant cooling arrangements might improve pipe temperatures but have minimal impact on overall cycle efficiency.

Keywords: Advanced ultra-supercritical plant, Thermal barrier coatings, Cycle efficiency, Pipe wall temperatures, Steel pipes

Nomenclature

Symbols

d_i	Inner pipe diameter
h	Enthalpy
$HARP$	Heating above the reheat point
L	Length of steam transfer pipe
p	Pressure
R	Thermal resistance
s	Entropy
T	Temperature
w	Width
$\dot{m}$	Mass flow rate
$\dot{Q}$	Heat transfer rate
$\dot{W}$	Power

Greek Symbols

α	Heat transfer coefficient
η	Efficiency
λ	Thermal conductivity

Subscripts

co	Coolant
fw	Feedwater heater
in	Inlet
$isen$	Isentropic process
out	Outlet
$pipe$	Pipe
TBC	Thermal barrier coating
wf	Working fluid

Superscripts

Sat	Saturated conditions

1. Introduction

There is an increasing demand to achieve higher efficiency in steam turbine electrical power generating plant [1]. For this the temperature of the steam entering the turbine should be as high as possible and that leaving as low as practical. In response to this, designers are seeking to raise the operating temperatures above 600 °C and even up to about 700 °C. In general, advanced ultra super critical plant (A-USC) achieve cycle efficiencies as high as 55%, far more than the cycle efficiency of about 40% in typical conventional plants [1]. Similar aspirations are under consideration for the next generation of nuclear electrical power generating plant, referred to as GEN IV [2]. However, in these cases in addition to higher temperature for increased efficiency, there is the potential for producing hydrogen. Certainly hydrogen is an option for replacing fossil fuels for a range of applications. In this context higher temperature nuclear reactors would enable both thermochemical and high temperature electrolysis options to be pursued. It is noteworthy that even some designs of Pebble Bed reactors have incorporated a steam generator and a maximum reactor outlet temperature of 750 °C. Such service conditions place severe demands on the materials and limit those potentially available that can be selected for specific components in future plant [3]. For existing power plant operating at higher temperatures the components are fabricated from a range of steels, including ferritic / martensitic high alloys such as P91 and austenitic stainless steels like Type 316 L. Unfortunately, the alloys suitable for the required greater temperature applications are limited to the higher cost austenitic stainless steels and nickel base alloys, such as Inconel 617, to ensure that the required mechanical properties, creep strength and corrosion resistance are sufficient to provide practical design service lives [4, 5, 6].

Hence it is important to explore alternative engineering design options that would allow existing ferritic and austenitic stainless steels to be selected. These steels are known to have good service performance at lower operating temperatures, below 600 °C, enabling the lives of approximately 40 years to be achieved with high confidence [3].

In this paper we consider a design for steam transport pipes and tubes that would allow the temperature experienced by these components to be reduced by use of a Thermal Barrier Coating (TBC), whilst achieving the design temperatures necessary for the thermal efficiency. Thermal barrier coatings are thermally insulating layers made of low thermal conductivity ceramics. They are used to increase the operating temperature or reduce cooling require-

ments in gas-turbines [7, 8, 9] and diesel engines [10]. The use of TBCs and internal cooling can provide temperature reductions of 100 °C to 300 °C allowing gas-turbine blades to operate at temperatures above the blade material's melting temperature. There are a range of different ceramics used for TBCs, with yttrium stabilised zirconia being widely used [11] and chosen for this study. There are many different methods for applying TBCs [12]. For example, coating thickness of about 4 mm can be achieved using solution-precursor plasma spraying[13].

TBCs have not previously been employed in any steam plant; the idea is novel. A related concept to reduce pipe wall temperature is to adopt metal foil barriers [14], sometimes packed with Kaowool [15], in experimental helium loops. The experiments mimic the primary circuits in nuclear reactors, between core and steam generator, and for the relevant operating conditions bulk helium temperatures approach 1000 °C and pressures 40 bar.

The aim of this work was to explore the effect of TBCs on A-USC cycles. The context was a feasibility study to gauge the scale of undesirable energy loss and the scale of beneficial reductions in pipe wall temperatures. Only if the losses and wall temperatures were likely to be within reasonable limits could we consider detailed further work and modelling, the scope of which comprises a topic in the discussion section. The concept is sketched on Figure 1 where the coating is applied to the inner surface of the transport pipe. The necessary cooling of the external surface of the transport pipe is derived from turbine exhaust steam or turbine bleed steam. The objectives of the current work were to estimate (1) the effects of the TBC arrangement on cycle efficiency (2) the effects of the TBC arrangement on pipe wall temperatures (3) the further effects of changes in plant operating pressures and temperatures (4) the further effects of changes in plant layout.

To this end a hypothetical plant was postulated. A regenerative cycle with reheat [16] was modelled with and without the addition of the TBC arrangement, at realistic A-USC pressures and temperatures. To derive the cycle efficiency a mathematical model was applied to thermal barrier coated zones of steam pipework and the associated heat transfers, employing steady-state balances of heat and material at all plant items. Five cooling arrangements were considered with reference to; practicability of plant layout, cycle efficiency, wall temperature and steam pressure loss; most arrangements ensured that the reduction in cycle efficiency was less than 1% and some arrangements succeeded in keeping surface temperature below 600 °C.

2. The Plant

The aim in this paper is to assess the thermodynamic feasibility of using thermal barrier coated steam pipes along with cooling, so that steam temperatures higher than the material limit can be used. In this section we hypothesise a relatively simple plant with sufficient components to test our aim and objectives. This section offers a broad outline of the plant in two stages: *without* (Figure 2) and *with* (Figure 3) a novel arrangement for cooling transport pipes. The plant without cooling is referred to as the "customary" plant in the rest of this paper.

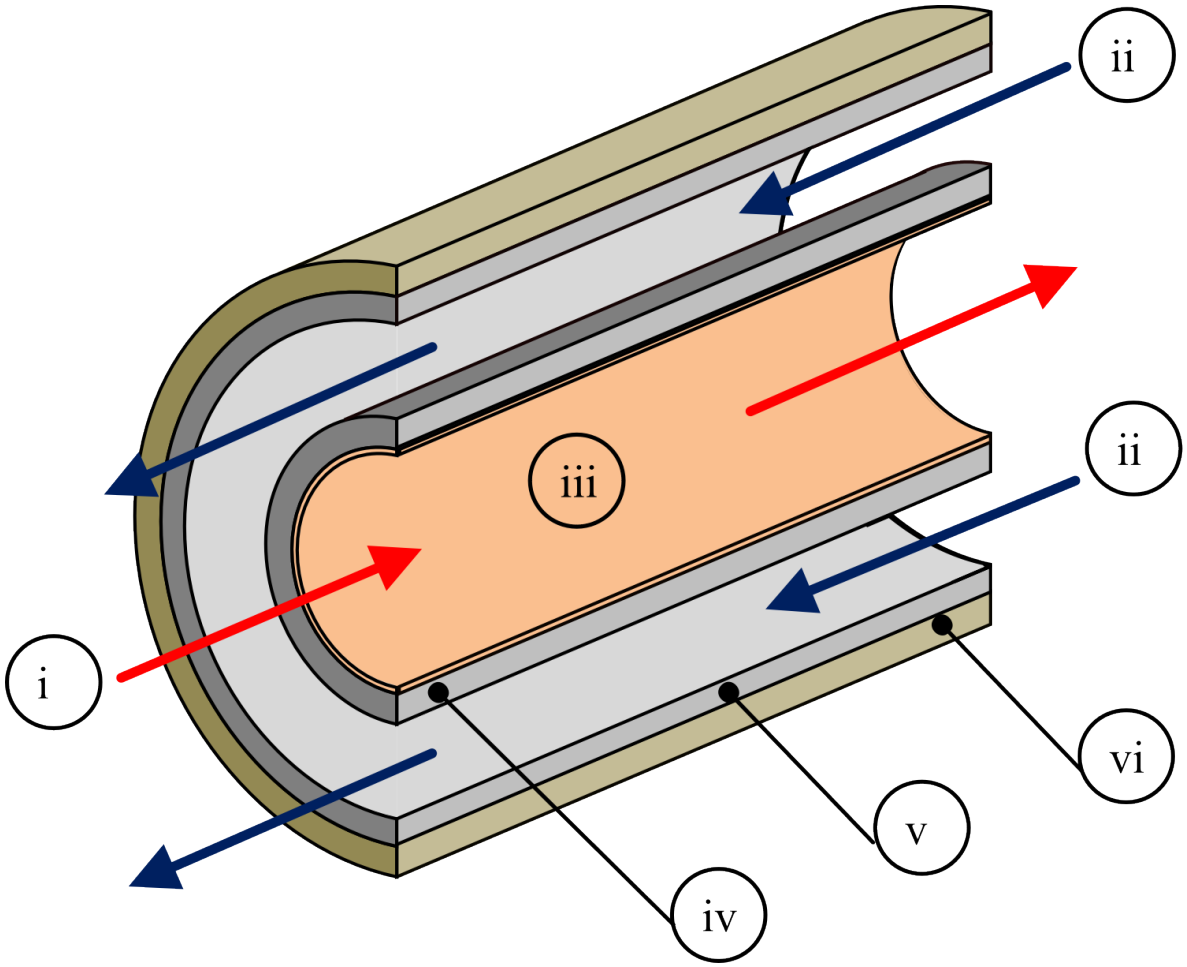

Figure 1: A cooled steam pipe (i) flow of working steam, (ii) countercurrent flow of cooling steam (iii) thermal barrier coating (iv) steam pipe proper (v) outer jacket (vi) insulation.

.

Figure 2 shows a supercritical, regenerative cycle with single reheat. Following current practice, the transport pipes are not cooled. The transport pipes in question are shaded grey, and labelled "pipe1" and "pipe 2". There are three features common to A-USC plant [4]. (1) The "boiler", shown here as a single unit, produces supercritical steam. (2) Regenerative heating is exploited. At three bleed points a fraction of the turbine steam is taken to heaters that serve to raise the temperature of the boiler feedwater, to the advantage of cycle efficiency. (The feedwater train is the simpler form used in [16], rather than the longer trains of reheaters used in the simulations of [4].) (3) Steam is heated a second time, in a reheater, before passing to the low pressure (LP) turbine.

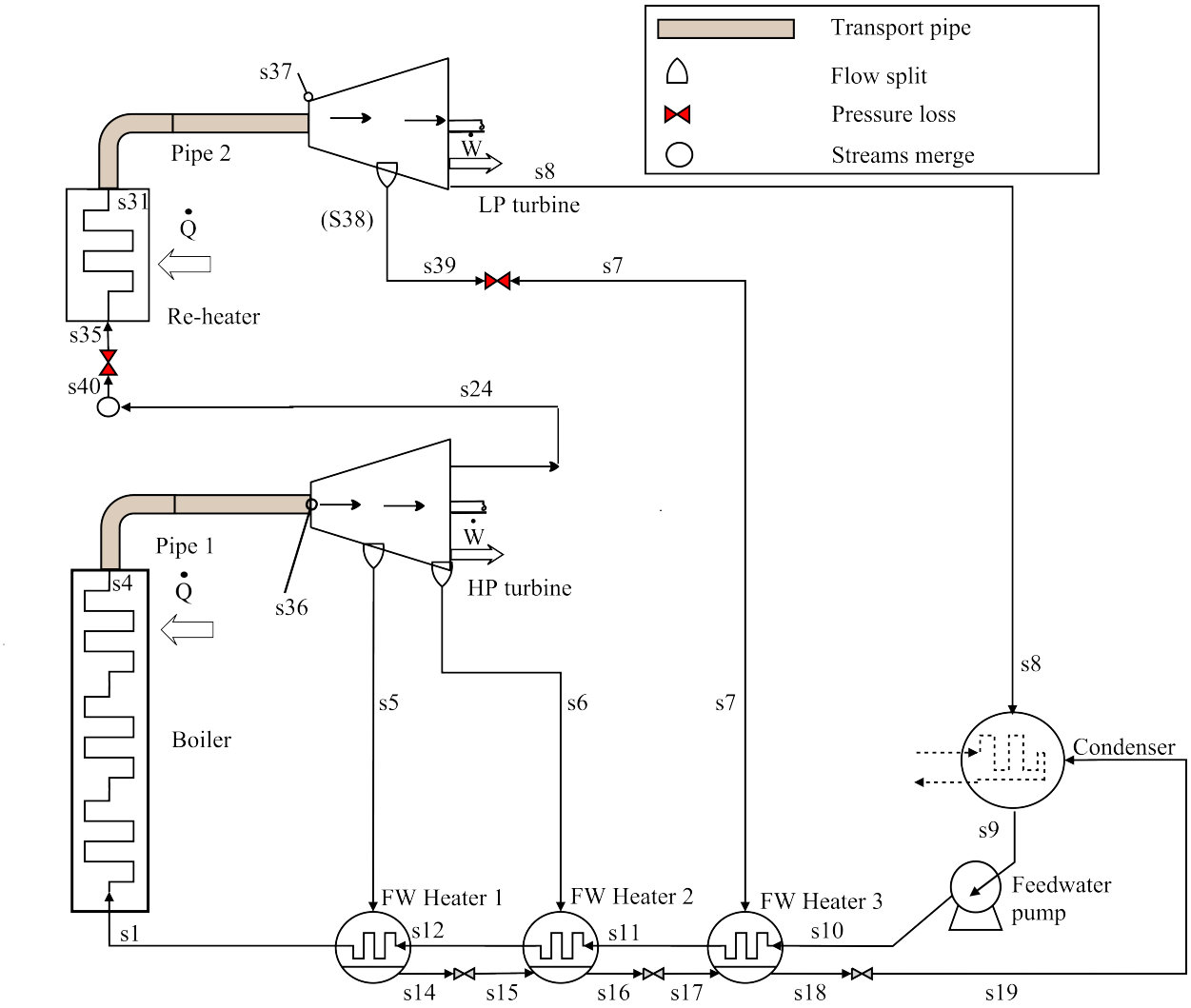

Figure 2: Supercritical Cycle with Reheating and Regenerative Feedwater heating [16].

.

Figure 3 shows the same plant modified with thermal barrier coated counterflow components. The high pressure transport pipe was coated (TBC1) and a cooling jacket was fitted. The original direct connection of the turbine exhaust to the reheater (See Figure 2) was diverted, to pass steam through the cooling jacket for the transport pipe and cool TBC1. Likewise the direct connection from the LP turbine bleed (stream s38) to feedwater heater 3 was diverted so as to cool the low pressure transport pipe and TBC2.

The more detailed aspects of the regenerative heating follow, common to Figures 2 and 3. The steam supplied to the feedwater heaters (through streams s5, s6, s7) condenses and releases its heat of vaporisation to the feedwater. The condensate, at comparatively high pressure, needs to pass through throttles so as to be at the same pressure as the condenser. (For the purposes of this paper, discussion of a de-aerator at intermediate pressure is omitted.) Note that, for example, steam bled from the exit of the HP turbine (stream s6) is at the reheat pressure and the feedwater

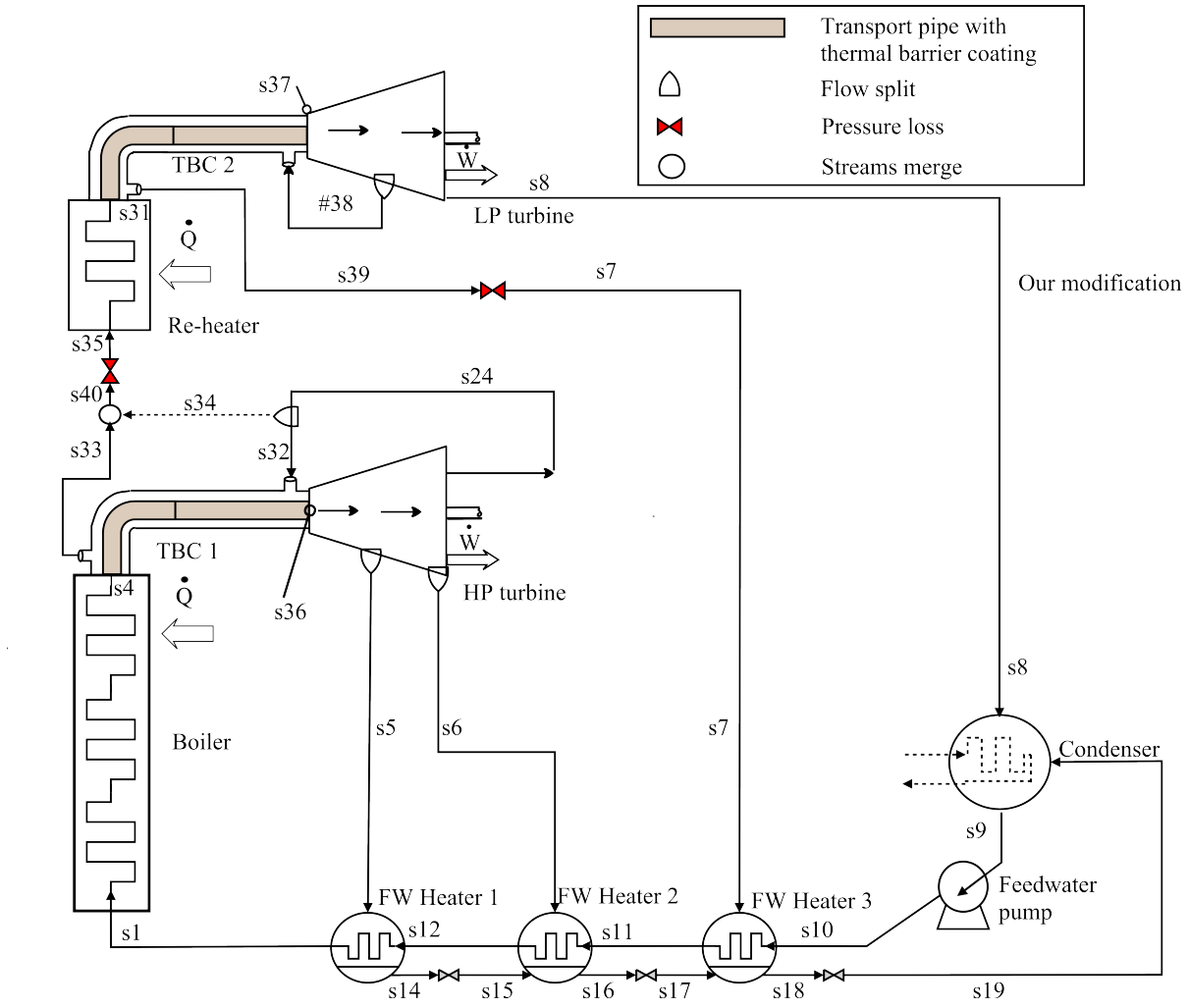

Figure 3: Cycle shown in Figure 2 with steam diverted so as to cool transport pipes. In the case shown in Figure 2 stream s24 was connected directly to the reheater and stream s38 was connected directly to Feedwater Heater 3

is (in principle) brought to the corresponding saturation temperature, $T_{12} = T_{sat}(p_6)$ on Figures 2 and 3. Raising the feedwater to a higher temperature is termed "Heating above the reheat point" (HARP) and hence feedwater heater 1 is a HARP heater in both plants.

Baseline simulation conditions were set as follows. The boiler pressure (350 bar), superheater temperature (700 °C) and reheat temperature (720 °C) were those identified as "future conditions" in the European Union Thermie/AD700 programme [17], aiming to develop new superheater and turbine materials and targeting an overall net plant efficiency of over 50%. The selection of a reheat temperature slightly greater than the "superheat" temperature accords with a review [1] of existing A-USC plant operating in five geographic regions. Superheat boiler exit temperatures ranged from 568 °C to 603 °C and reheater temperatures were consistently 8 °C to 28 °C higher (in the range 596 °C to 623 °C). The length of transport pipe (200 m) was similar to that used in UK conventional plant as was the pipe bore and thickness (0.24 m and 0.06 m respectively).

It should be noted that true pipe runs are complex - e.g. four pipes from the boiler joining in a steam chest to form a single pipe. A single pipe suffices for the purposes of the current work. The baseline 200 m is represeantative of several coal-burning, subcritical plants in the UK generating in the region of 500 MWe (personal communication from Mr Andrew Morris, Fleet Chief Mechanical Engineer, EDF Energy, Nottingham). Each boiler feeds four main steam legs rising to a steam chest from which a single pipe emerges. Our *baseline* condition takes the same steam mass flow rate, pipe bore and pipe thickness as in each of the steam legs. The length of the steam legs will be taken up by most of the boiler house, in the region of 50 to 75 m tall, plus a length of entry into the turbine hall. After the steam chest and feeding the turbine, a section of model that in effect merges four pipes into one larger pipe would reduce the available heat transfer area per unit mass flow of steam. The single-pipe approximation tends to render the estimated heat losses pessimistic and therefore conservative. In the results section pipe length is surveyed and the discussion section covers the pipe length in future steam generators. The potential mass of superalloy in the transport pipe might well be compared with superalloy that must be used in the boiler and reheater. Weitzel's detailed design of a component test steam generator [18][19] indicates 1 tonne of superalloy per generator for each 1 kg/s of steam flow and roughly the same as in each of the two transport pipes.

The reheat pressure was 75 bar [1]. The assumed rate of flow through the boiler was 100 kg s^{-1}, yielding a baseline electrical power output of 148 MWe; this compares with production for many UK conventional plant in the region of 500 MWe (or 125 MWe attributed to each of four steam pipes). Isentropic efficiencies were set to 90% for all turbines. For simplicity, unless stated otherwise, the results are without HARP; that is no heat was transferred in the highest pressure feedwater heater 1 for either plant. The temperature of condensation was taken as 29 °C, similar to UK conditions. The coating thickness applied to TBC1 and TBC2, Figure 3, was set at between w = 0 mm and w = 5 mm. The value of w = 4 mm thickness was the thickest layer achieved previously [13] with peer review. The use of 5 mm thick layers for industrial gas-turbine engines is also mentioned, without reports of any measurements or analysis[20].

3. Thermodynamic Modelling of Plant

The important parameters are the cycle efficiency of the plant and the maximum pipe surface temperatures in the transport pipes. This section covers the associated material and energy balances, the calculation of radial temperature profiles through the transport pipes to provide the maximum surface temperatures, and the overall calculation procedure for the plant.

3.1. Energy Balances

The cycle efficiency of the plant, η_{cycle}, is the ratio of net power output to heat input given by,

$$\eta_{cycle} = -\frac{\sum \dot{W}_j}{\sum max(0, \dot{Q}_i)} \tag{1}$$

where $\dot{W}$ and $\dot{Q}$ are the work and heat transfer of each plant item respectively. The max operator acts to exclude heat rejection from the condenser. The heat transfer and work done by each plant item was calculated from the Steady Flow Energy Equation, [16],

$$\sum_{i=1}^{I} \dot{m}_{out,i} h_{out,i} - \sum_{j=1}^{J} \dot{m}_{in,j} h_{in,j} = \begin{cases} \dot{W}, & \text{if turbine or pump} \\ \dot{Q}, & \text{if fluid is heated or cooled} \\ 0, & \text{otherwise} \end{cases} \tag{2}$$

where $\dot{m}$, h, $\dot{W}$ and $\dot{Q}$ are the mass flow rate, enthalpy, power and rate of heat transfer respectively. The subscripts *in* and *out* correspond to the number of streams, J, that enter each plant item and the number of streams, I, that exit it. To calculate the power and the heat transfer, the mass flow rate and enthalpies were determined for each plant item. The mass flow through each plant item has to satisfy the conservation of mass,

$$\sum_{i=1}^{I} \dot{m}_{out,i} = \sum_{j=1}^{J} \dot{m}_{in,j} \tag{3}$$

All plant items except pipe t-junctions and the condensate side of each FW heater have a single inlet and outlet, so Equation 3 often simplified to $\dot{m}_{in} = \dot{m}_{out}$. The enthalpy for supercritical and superheated steam was found according the state postulate; thus it can be calculated from two other properties from pressure, p, entropy, s, or temperature T. For saturated steam or saturated water only a single known state property is needed to calculate enthalpy and the remaining properties. The XSteam Matlab function [21] was used to calculate thermodynamic properties of steam; XSteam implements the IAPWS97 formulation [22] for the temperatures from 0 °C to 1000 °C and the pressures from 0.0061 bar to 1000 bar.

The plant operating conditions, given in Section 2, were used to define some of the plant states. To obtain the state properties at other plant locations some processes were assumed to be isobaric ($p_{in} = p_{out}$), isenthalpic ($h_{in} = h_{out}$) or

isentropic ($s_{in} = s_{out}$), as summarised in Table 1.

Table 1: Assumed plant behaviour (assumptions indicates by ✓)

Item	Isobaric $p_{in} = p_{out}$	Isenthalpic $h_{in} = h_{out}$	Isentropic $s_{in} = s_{out}$
Boiler, reheater	✓		
Valve		✓	
Split	✓	✓	✓
Merge	✓		
Turbine			✓(First calculation step)

To calculate the change in enthalpy across a turbine, the turbine was initially assumed to be isentropic $s_{in} = s_{out}$, with the exit enthalpy $h'_{out} = h(p_{out}, s_{in})$. The energy equation, Equation 2, then gave the isentropic power developed by the turbine which was corrected using, $\dot{W} = \eta_{isen}\dot{W}_{isen}$, to give true power and thus the true outlet enthalpy [16]. The calculation of the change in enthalpy for the FW heater and the TBC pipes involved solving for the internal heat transfer and are described in more detail below.

3.2. Feedwater Heater

The control surface around a feedwater heater is shown in Figure 4. This represents any of the three feedwater heaters on Figure 3. Heat addition $\dot{Q}_{TBC}$ (through TBC 2) applies to FW heater 3 only and is absent for FW heaters 1 and 2. The associated pressure and temperature changes from b to bc are attributed to the cooling duct and hence are nonzero for FW heater 3 and zero for FW heater 1 and 2. The control volume features an inlet flow of high pressure boiler feedwater (labelled F) from either the condenser (to FW heater 3) or an adjacent FW heater, a physically separate inlet flow of condensate from an adjacent heater (labelled D), a turbine bleed stream (labelled b), the bleed stream after any pressure loss and heat transfer prior to FW heater 3 (labelled bc), a sump that drains to the adjacent, lower pressure heater or the condenser (label D_e) and the feedwater outlet. The control surface was drawn to allow for any heat transfer to the coolant in the TBC pipe, $\dot{Q}_{TBC}$. Inside each FW heater the bleed steam transfers heat to the feedwater by condensing on the outside of a heat transfer coil. The sump inlet and outlets are treated as saturated water. The underlying assumptions are that feedwater outlet/sump inlet are treated as being at the bleed steam saturation temperature, $T_{F,out} = T_D = T^{Sat}(p_{bc})$, and that the sump inlet and bleed steam inlet pressures are equal, $p_D = p_{bc}$[16]. The mass flow rate in the sump exit stream is $\dot{m}_{De} = \dot{m}_D + \dot{m}_b$. Combining the above assumptions with Equation (2) the required mass flow of bleed steam, $\dot{m}_b$, is given by

$$\dot{m}_b = \frac{\dot{m}_F \left\{h(T_{F,out}, p_F) - h(T_{F,in}, p_F)\right\} + \dot{m}_D \left\{h^{Sat}(p_{be}) - h^{Sat}(p_{bc})\right\} - \dot{Q}_{TBC}}{h_b - h^{Sat}(p_{be})} \tag{4}$$

The feedwater heaters were configured to achieve a constant temperature gain across feedwater heater 2 and 3, $T_{fw,out} - T_{fw,in} \widehat{=} T_{12} - T_{11} = T_{11} - T_{10}$. This corresponds to a constant enthalpy drop ($h_b - h_{fw,out}$) described by

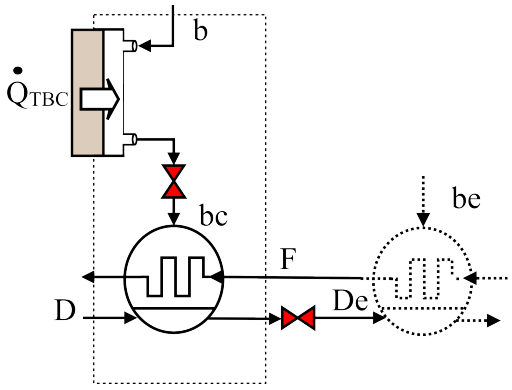

Figure 4: Control volume for heat balance on feedwater heater (detail given in text)

Salisbury[23] that results in optimum cycle efficiency [24]. Were steam to be superheated throughout the high pressure turbine, the associated optimum heater-to-heater enthalpy drop would be typically 1.5 to 1.8 times higher than that in the low pressure turbine [25]. The special instance of supercritical steam at the HP turbine inlet would necessitate computational optimisation of the bleed points. One should note that extraction of feedwater heating fluid from the high pressure turbine (through stream s5, Figure 3) is termed Heating Above the Reheat Point (HARP) [24].

3.3. The Coated Steam Pipes

The TBC pipes acted as a counterflow arrangement, Figure 1 to transfer heat from the *working fluid*, intended to drive the turbine, to the *coolant fluid*. An energy balance over the dual pipe yielded the coolant exit enthalpy and thus the coolant exit temperature. For the purposes of the energy balance, the fluids were assumed to flow with no pressure loss.

Assuming that the heat transfer coefficients are independent of the length of the pipe, the heat transfer equation can be written [16] to give the length of the pipe, L, as:

$$L = \frac{\sum_{k=1}^{4} R_k}{\frac{\theta_{in}-\theta_{out}}{ln(\theta_{in})-ln(\theta_{out})}} \dot{Q}_{TBC} \tag{5}$$

where $\theta = T_{wf} - T_{co}$ is the temperature difference between the working fluid and the coolant, the subscripts (in, out) refers to locations in the working fluid, the denominator group is the logarithmic mean temperature difference and R_k is a set of thermal resistances, R, given below and the locations are shown in Figure 5. The thermal resistances per unit length of coated pipe, R, were given by

$$R_1 = \frac{1}{\pi(d_i - 2w_{TBC})\alpha_{wf}} \tag{6}$$

$$R_2 = \frac{ln(1 - 2w_{TBC}/d_i)}{2\pi\lambda_{TBC}} \tag{7}$$

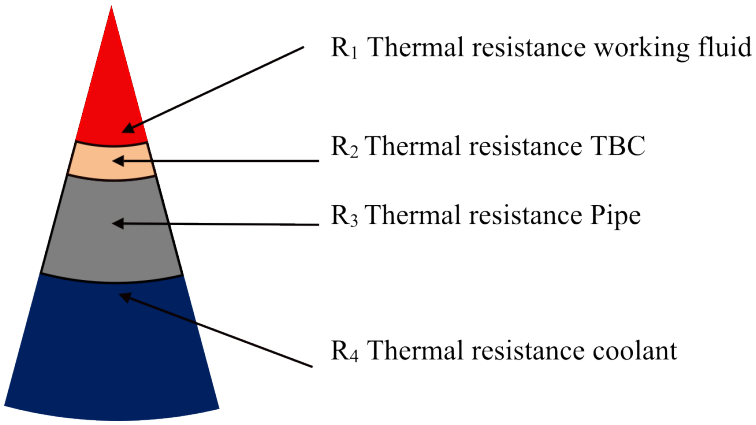

Figure 5: Thermal resistances calculated for TBC pipes (see equations 6 to 9).

.

$$R_3 = \frac{ln(1 + 2w_{pipe}/d_i)}{2\pi\lambda_{pipe}} \tag{8}$$

$$R_4 = \frac{1}{\pi(d_i + 2w_{pipe})\alpha_{co}} \tag{9}$$

where α and λ represent heat transfer coefficients and thermal conductivities respectively, w is the thickness of thermally coated zone or tube wall and d_i is the inner diameter of the steel pipe.

Reviews of the heat transfer coefficients of supercritical steam, α_{ws}, are found in papers by Jackson [26] and Wang [27]. Although buoyancy effects have been discussed in the previous references these were neglected from this analysis as the coolant and working fluids have Richardson numbers below 10^{-5} [26] for both pipes. The heat transfer coefficients can change sharply with distinct peaks in physical properties near the pseudo-critical line. We used the correlation of Yamagata et al [28] which yielded α_{ws} within ±20% of experimental data. The Nusselt number was correlated against Reynolds and Prandtl numbers plus a correction F_c. The term F_c was computed from pseudo-critical, wall and bulk physical properties according to the Eckert number. Data for the supercritical line is taken from Pioro and Mokry [29] which provides tabulated values up to 350 bar.

Yttrium stabilized zirconia was chosen as the thermal barrier coating based on Stoever and Funke's review [30] of the composition and stability of thermal barrier coatings typically used for small components such as turbine blades. The thermal conductivity of yttrium stabilized zirconia is $\lambda_{TBC} \in [1.1, 1.5] Wm^{-1}K^{-1}$ in the range from 900 °C to 1320 °C [11]. For the thermal conductivity of pipe walls, λ_{pipe}, data for 9Cr-1MoVNb steel from reference [31] were taken as representative of P91 steels [32]. The heat transfer coefficient of the coolant, α_{co}, was computed using the Nunner correlation, reported in [33]. The correlation employs smooth-surface and rough-surface friction factors. The rough surface friction factors were found using an approximate solution to the Colebrook equation [34].

Once the thermal resistances, R, and coolant outlet temperature had been established, the pipe wall surface temper-

atures were evaluated. At a given axial co-ordinate, the thermal resistances enable the estimation of the temperatures of the inner and outer surfaces of the pipe, $n = 2$ and $n = 3$ respectively, using the following equation:

$$T_n = T_{wf} + (T_{co} - T_{wf}) \frac{\sum_{k=1}^{n} R_k}{\sum_{k=1}^{4} R_k} \tag{10}$$

The pipe surface temperatures were calculated at the beginning and end of the steam pipes to find the maximum pipe surface temperatures.

3.4. Calculation Procedure and Tests

The working fluid temperature at the exit of the TBC pipes, $T_{wf,out}$, (T_{36} and T_{37} on Figure 3) was adjusted iteratively. Each iteration looped over the plant, solving for the plant state properties until all possible properties are found. The cycle efficiency and TBC pipe length were then calculated. The iterations were stopped when the computed and specified pipe lengths, L, matched. A summary of the calculation procedure is given in Figure 6.

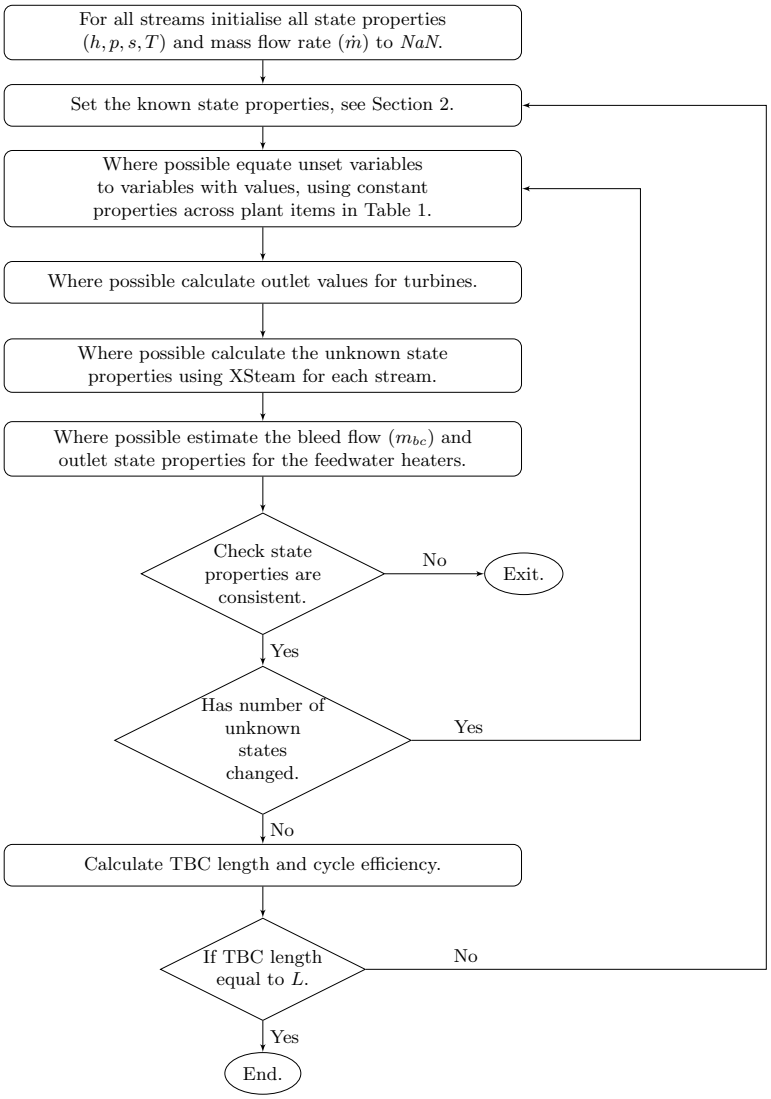

Figure 6: Flow diagram showing the steps in the calculation procedure.

.

To validate the calculation procedure two worked calculations of sub-critical regenerative cycles published in [16] were repeated. For a basic regenerative Rankine cycle with a single bleed the calculated cycle efficiency agreed exactly with the published value of 37.3 % [16]. For a Rankine cycle with reheat and three bleed points the calculated cycle efficiency was 40.9 % versus 41.0 % estimated in [16].

Few published predictions of supercritical plant provide sufficient detail for checking and verification. Comparisons with [4] were promising, notwithstanding differences in plant set-up and the omission of certain details in their original paper such as assumed pressure losses in pipes, isentropic efficiencies of turbines, and their baseline efficiency (from which all cycle efficiencies could be derived, using their reported heat rate improvement).

4. Results

Simulations start with the baseline conditions (identified in Section 2), both with "customary plant" which provides a reference condition, and with arrangements for thermal barrier coating and countercurrent cooling. We investigated sensitivity of these estimates to process and plant parameters, and adjustments to plant configuration. In the course of the analysis it became evident that pressure losses were important, particularly in the jacket attached to the lower pressure transport pipe (TBC 2, Figure 3). The final part of this section thus investigates the effect of pressure losses.

4.1. Baseline Conditions

The baseline conditions were applied to a customary plant and to a plant with cooled transport pipes. Figures 7 (a) and (b) show the predicted cycle efficiencies for the customary plant with transport pipes uncooled. (The plant is shown on Figure 2) . Wall temperatures would be close to the working steam temperatures of 700 °C in the high pressure pipe 1 and 720 °C in the low pressure pipe 2. In Figure 7 (a), cycle efficiency increased with throttle pressure p_4 (no HARP was applied here). Figure 7 (b) shows the effect of reheat pressure - tests were carried out with and without HARP. Regardless of whether or not HARP was applied, the baseline reheat pressure (p_{35} =75 bar) yielded cycle efficiencies close to maximum. The HARP, when applied, raised the feedwater temperature to 372 °C and within 2 °C of the critical temperature. The increase in cycle efficiency - 0.45% - broadly indicates the scale of efficiency gains that plant designers consider worthwhile. For the conditions set up for Figure 7 the quality of the low pressure (LP) turbine exhaust changed only with the reheat pressure. The quality was 95.6% at 30 bar and decreased to 88.4% at 110 bar. At the baseline reheat pressure of 75 bar (applicable to Figure 7, part (a)) the quality was 90.9%.

Modified calculations dealt with the two transport pipes being coated, jacketed and cooled (as per Figure 3). Figure 8 shows the radial temperature profiles through the highest pressure pipe (TBC 1 on figure 3), at both ends of the pipe, highlighting the critical temperatures at the pipe walls. The bulk supercritical steam is point 1, the bulk coolant is point 5 and the pipe is hottest at the pipe-ceramic interface (point 3). Two observations follow. First, most of the temperature drop was though the solid surfaces (the TBC, 2-to-3, and the steel, 3-to-4) and very little temperature drop was through the boundary layers (1-to-2 and 4-to-5). Second, the bulk temperature of the supercritical steam was reduced from 700 to 683.7 °C to the detriment of cycle efficiency.

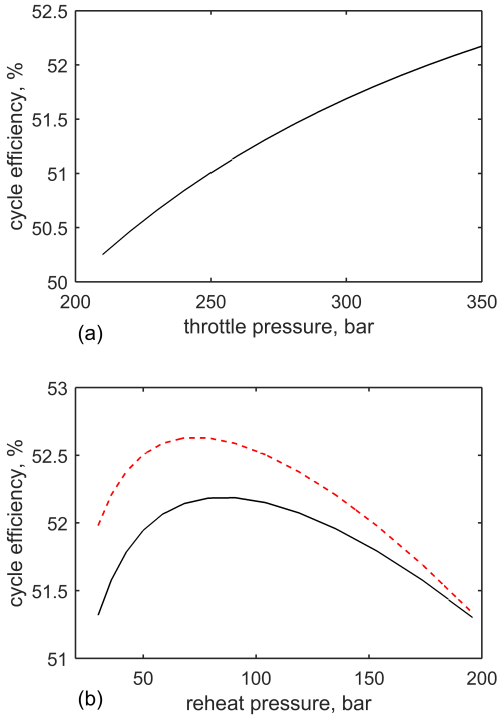

Figure 7: Cycle efficiencies for "customary plant" (Figure 2)) (a) impact of throttle pressure (no HARP is applied)(b) impact of reheat pressure: ——— No HARP; - - - - - - - with HARP. Baseline conditions include throttle pressure = 350 bar, reheat pressure = 75 bar

.

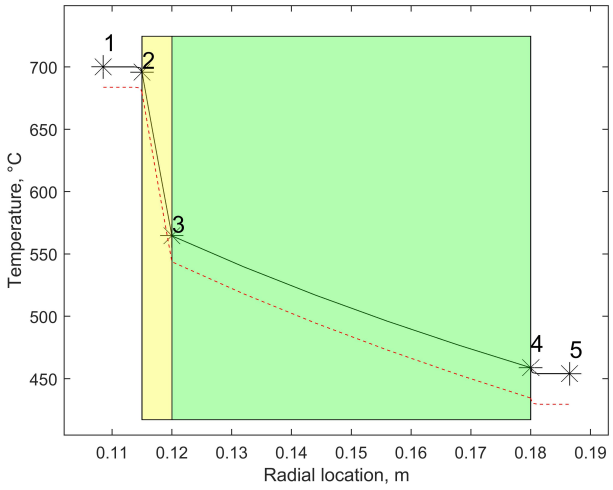

Figure 8: Radial profiles of temperature at in the high pressure transport pipe (TBC 1, at 350 bar and under baseline conditions). The TBC is shaded yellow and the pipe wall is shaded green. Thus, point 1 is the steam bulk temperature, point 2 is the inner edge of the ceramic layer, point 3 is the TBC-pipe interface, point 4 is the outer edge of the pipe, point 5 is the coolant bulk temperature. Coating thickness is $w = 5$ mm; ——— inlet plane, x=0 - - - - - - outlet plane, x=L

Thinner coatings resulted in higher temperatures, particularly at the TBC-to-pipe interface where the pipe temperature was at its maximum (see point 3 on Figure 8), as shown in Figure 9. Temperatures below target (600 °C) were achieved in the high pressure pipe (TBC 1) with w <2.8 mm but for the low pressure pipe (TBC 2) the necessary thickness of $w = 6.7mm$ (by extrapolation) exceeded that in current practice.

Figure 10 shows how much the coating thickness reduced cycle efficiency. The top (dotted) line shows the cycle efficiency for the customary plant (Figure 2) without cooling jackets, 52.4%. In this instance, pipe temperatures would equilibrate to the steam temperature necessitating adopting a high temperature alloy. The middle (solid) line shows the novel arrangement (Figure 3); the efficiency was reduced by 0.8% to 51.4% at w = 5 mm. The lower line shows results for a cooling system with no recovery of heat within the plant; in effect coolant would be supplied from outside the cycle and exhausted to outside the cycle. To obtain the same cycle temperatures the plant would require an additional amount of external heat $\dot{Q}_\delta$ to the detriment of cycle efficiency (η_{cycle} in Equation 1) given by

$$\dot{Q}_\delta = \dot{m}_{32}(h_{32} - h_{33}) + \dot{m}_{38}(h_{38} - h_{39}) \tag{11}$$

where the subscripts refer to stream numbers on Figure 3.

In summary of the baseline example, the best cycle efficiency was 51.4% and 0.8% less than the efficiency with customary transport pipes of 52.2%. Wall temperatures in the low pressure pipe (TBC 2) exceeded the limit of 600 °C by ≥ 17 °C. This temperature might be acceptable for some lower cost steels (possibly with modest modification to the steel composition), or in future years more effective internal insulation schemes might be developed. The rest of this paper considers alternative actions. Plant parameters are adjusted such as either the reheat temperature or the length of the transport pipe. Modifications to the baseline plant included (1) the use of a counter-current flow (2) supplying more coolant steam to the low pressure pipe (3) controlling the coolant flow rate to bring the wall temperature to a set point of 600 °C.

4.2. Changes to Plant Parameters

Temperatures in the lower pressure transport pipe (TBC 2) could be reduced simply by decreasing the reheat temperature. (See stream s31 on Figure 3). Figure 11 shows the consequences for the maximum pipe wall temperature and the cycle efficiency. A reduction in reheat steam temperature to T_{31} = 700 °C led to a tolerable surface temperature of 598.3 °C if w = 5 mm, and a cycle efficiency of 51.1%, only slightly below the baseline case (51.2%) and somewhat less than for customary transport pipes.

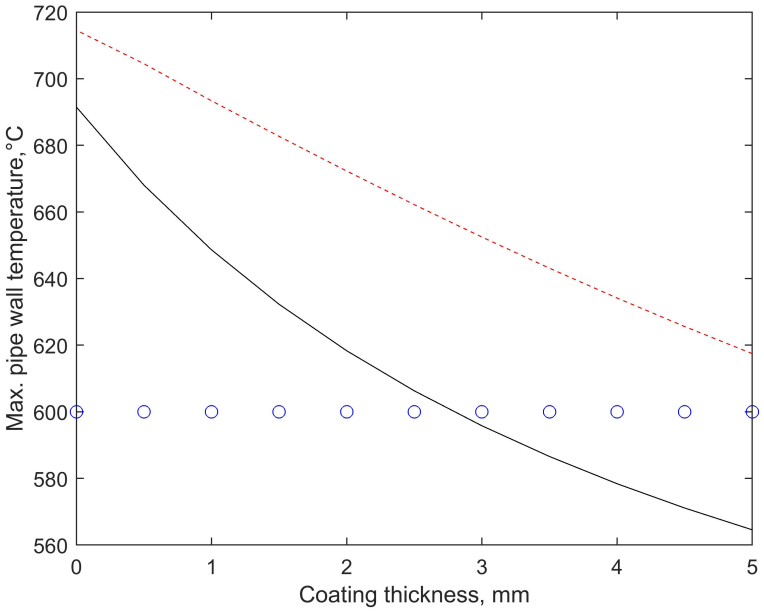

Figure 9: Effect of coating thickness on hottest pipe temperature (point 3 on Figure 8): ------ Low pressure pipe (TBC 2); ——— High pressure pipe (TBC 1); o target of 600 °C

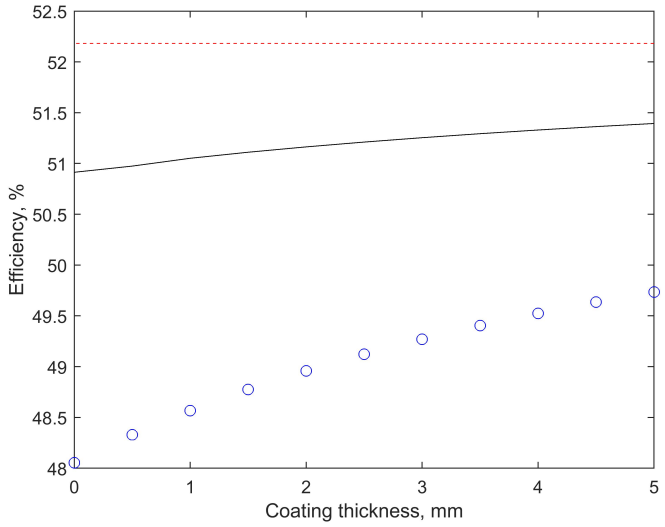

Figure 10: Effect of coating thickness on cycle efficiency: ------ customary approach with no TBC/ pipe cooling; ——— cooling applied, with heat recovered inside the plant; o cooling with no heat recovery

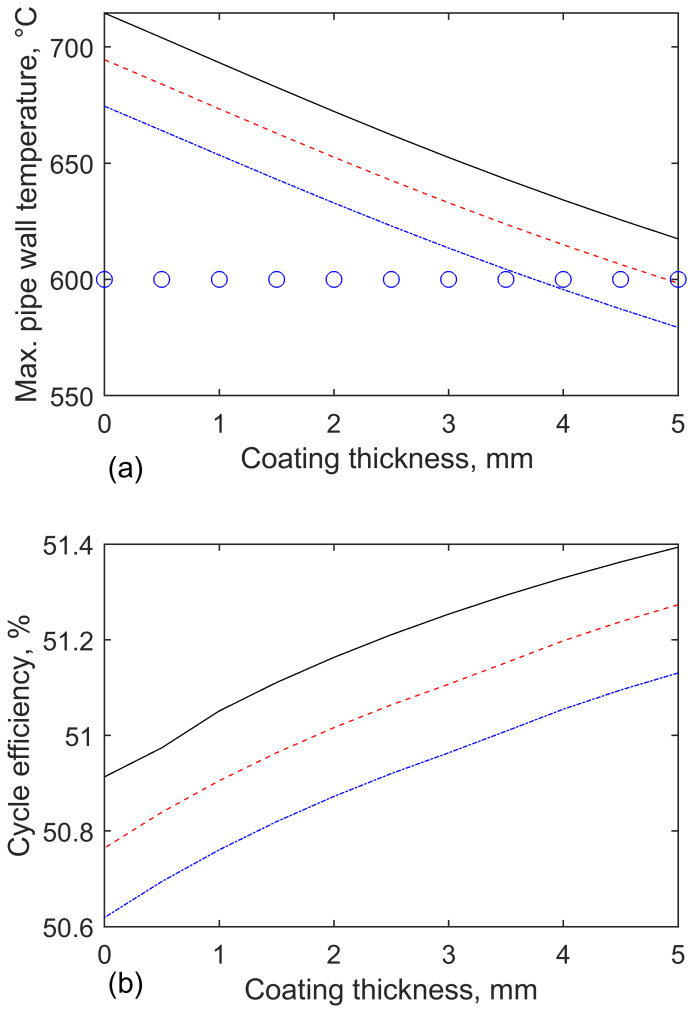

Figure 11: The effect of reheat temperature on (a) pipe wall temperature (lower pressure, TBC 2) and (b) cycle efficiency. Reheat temperatures are: ——— 720 °C; – – – – 700 °C ; ------- 680 °C. Symbol o indicates limit of 600 °C

The effects of the length of the TBC coated pipes on efficiency and surface temperatures are plotted on Figures 12 (a) to (c). The maximum surface temperature was at the working fluid inlet. Longer pipes resulted in reduced cycle efficiency owing to loss of heat from the working steam, Figure 12a. A pipe length of zero recovered the original efficiency of 52.2% for the customary condition, with no cooling system. Thicker coatings increased the cycle efficiency by reducing the heat loss from the working steam as well as reducing the maximum pipe wall temperature. For the first, high pressure transfer pipe a coating thickness of 2.5 mm was sufficient to keep the maximum surface temperature below 600 °C for all lengths explored, Figure 12b. For the second, low pressure transport pipe the thickest layer permitted pipe lengths up to 150 m (w = 5 mm and assuming the 600 °C limit). A thinner layer of 2.5 mm thickness permitted a pipe length of 25 m only, Figure 12c.

4.3. Modifications to Plant Layout

To address some of the issues identified several modifications to the plant were investigated. First, the baseline cooling to TBC coated pipe 1 was sometimes more than required, possibly to the detriment of overall cycle efficiency. So the plant was modified to keep the maximum pipe wall temperature at 600 °C by controlling the amount of steam used as coolant. Second, the direction of the coolant steam was changed from counter-current to co-current. This is because the thermal barrier coatings are more effective when there is a larger temperature difference between the working fluid and the coolant. Co-current cooling has the lowest temperature coolant at the same end of the pipe as the highest temperature working fluid. Third, to keep the temperature in TBC pipe 2 below 600 °C, the plant around the low pressure turbines was modified to make more steam available for cooling. Rather than condensing some coolant steam in feedwater heater 3, it was returned to a turbine. Details and results of the modifications are given below.

With regard to the first modification investigated, the temperature of the high-pressure pipe wall was controlled to a set point of 600 °C so as to minimise the required flow of cooling steam. To do this, a fraction of the HP turbine exhaust passed directly to the reheater (see stream s34, marked by the thicker line, on Figure 13 which represents a modification to Figure 3). Figures 14 (a) and (b) show, for the high pressure pipe (TBC1), surface temperatures and the mass flow rate of steam. Below 2.8 mm thickness the turbine exhaust provided insufficient steam, as coolant, to reduce the maximum pipe temperature below its target (see Figure 14 (a)). At 2.8 mm thickness the pipe wall temperature reached 600 °C using all the turbine exhaust steam. For thicker coating less steam was needed to keep the maximum pipe wall temperature at 600 °C (Figure 14 (b)). The best gain in efficiency (not plotted) was trivial at 0.029%.

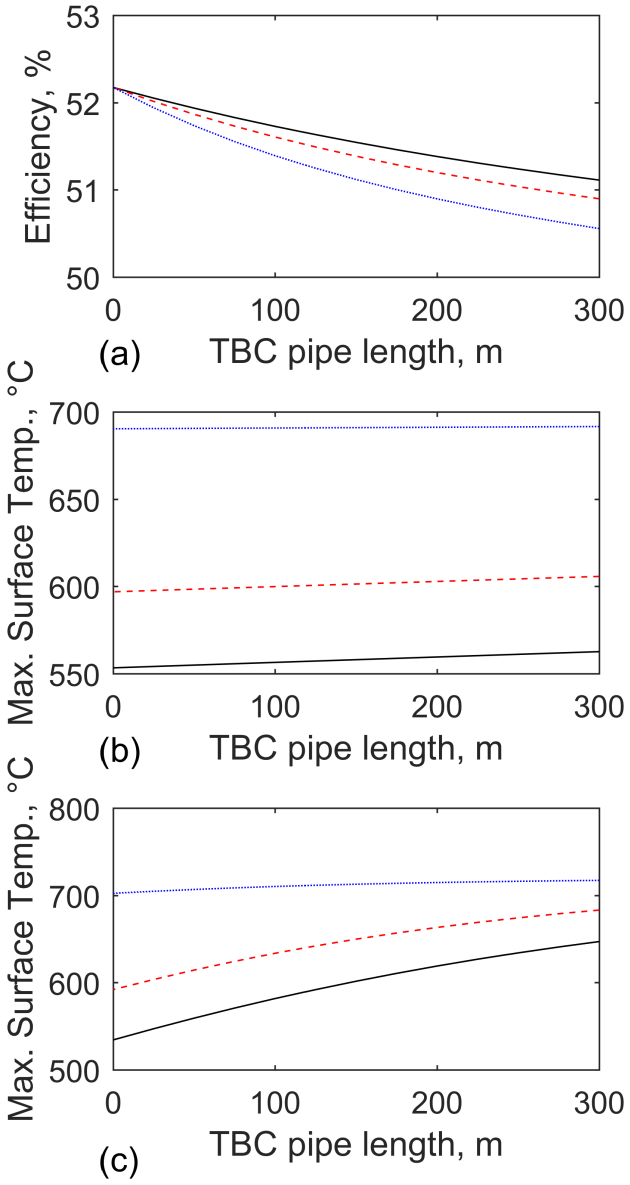

Figure 12: Effect of transport pipe length on (a) cycle efficiency (b) maximum surface temperature in the high pressure transport pipe (TBC 1) (c) maximum surface temperature in the low pressure transport pipe (TBC 2), for different coating thicknesses. Coating thicknesses are: ——— 5.0 mm ; – – – 2.5 mm ; ------- 0.0 mm

.

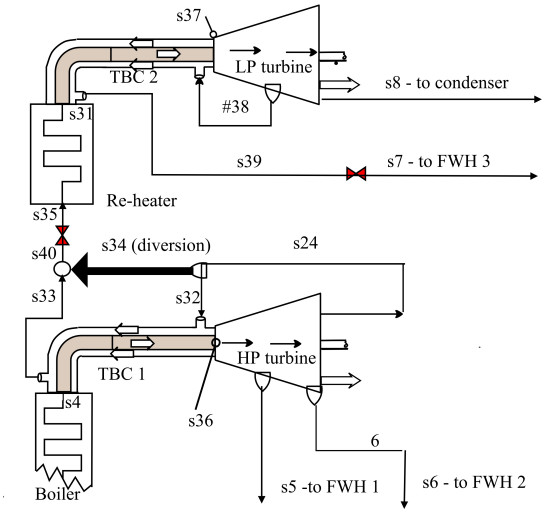

Figure 13: Alteration of the plant on Figure 3 to control flow through the high pressure transport pipe, TBC1. Stream s34 (thicker line), diverts some steam directly to the reheater, controlling the pipe wall temperature to 600 °C

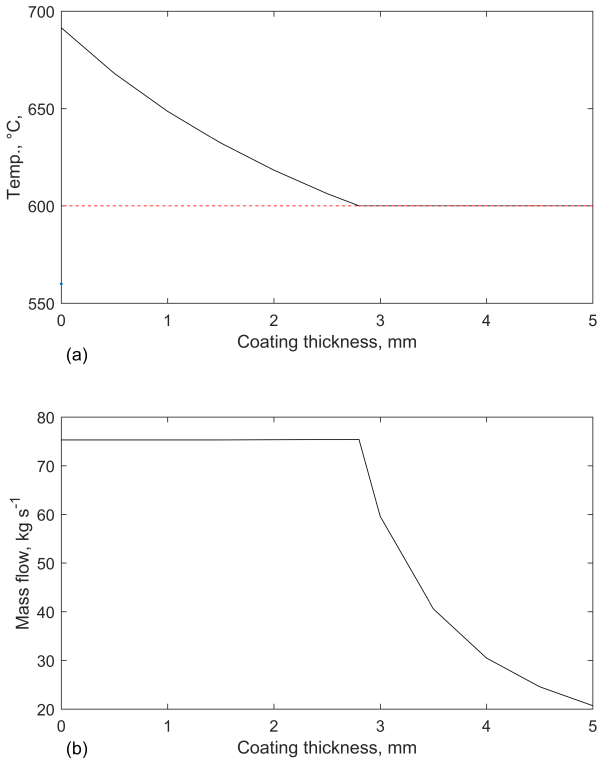

Figure 14: Controlled flow of coolant (applied to TBC1). (a) hottest surface temperature (see point 3 in Figure 8) ——— maximum temperature ; - - - - - - target (b) required flow of coolant through the cooling jacket

Another tactic concerned the cooling of transport pipes with a co-current flow. The modifications are shown in

Figure 15; they were applied to the baseline plant, Figure 3. Thus the coolant steam was introduced, at its lowest temperature, to the location where the working steam was at its highest temperature. For various thicknesses of TBC and for both steam transport pipes, Figures 16 (a)(b) show the wall surface temperatures at pipe inlet (x=0) and pipe outlet ($x = L$). For the thinner coatings ($w \rightarrow 0$ mm) the surface temperature tended towards that of the working fluid and was hotter at the pipe inlet (x=0), as was found for the counter-current case. On the other hand, for the thicker coatings ($w \rightarrow 5$ mm) the surface temperature tended towards that of the coolant and was hotter near the pipe outlet ($x = L$). At this point the coolant had accepted heat and increased in temperature. With regard to the target surface temperature of 600 °C, counter-current cooling of the high pressure pipe (TBC1) reduced the critical thickness of coating from $w = 2.8$ mm to $w = 2.1$ mm (baseline condition). Co-current cooling of TBC2 reduced the critical thickness from $w = 6.7$ mm to $w = 5.3$ mm. For any given thickness, the efficiency was practically unchanged from the baseline case. The efficiency gained 0.020% at $w = 0$ mm and lost 0.003% at $w = 5$ mm.

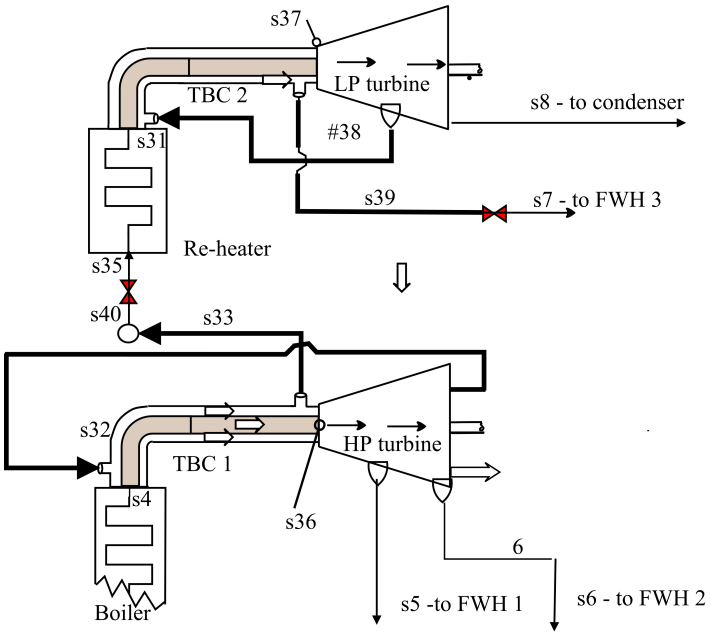

Figure 15: Co-current flow of coolant (applied to TBC1). Thick lines indicate new direction of flow

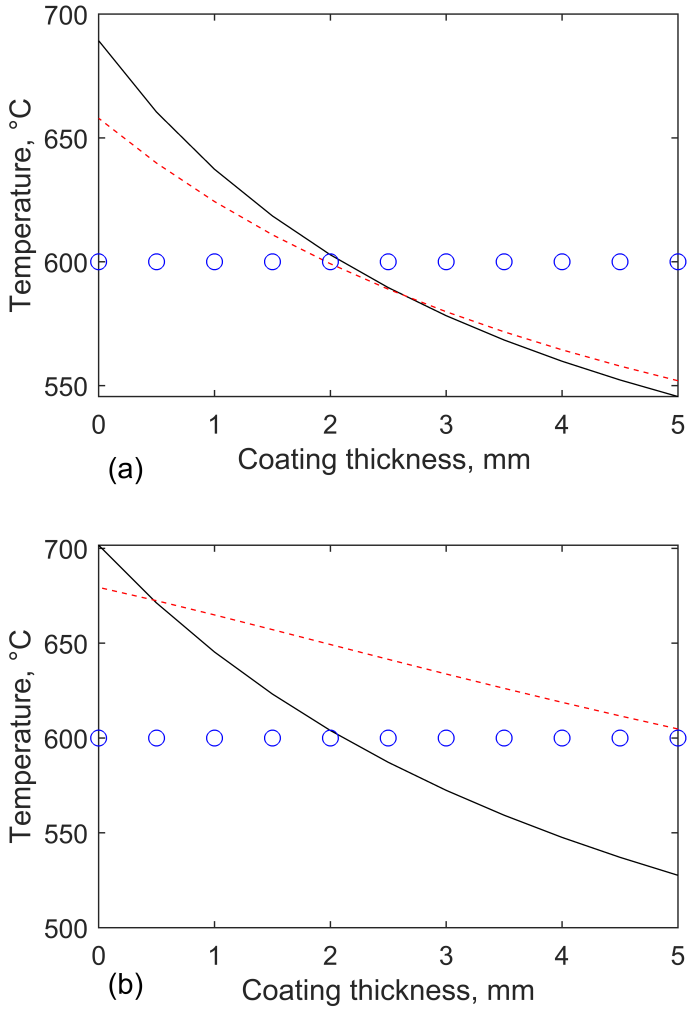

Figure 16: Pipe wall temperatures for co-current flow of coolant (a) higher pressure transport pipe, TBC1 (b) lower pressure transport pipe, TBC2: ——— at pipe inlet (x=0) ; - - - - - - at pipe outlet (x=L); o temperature limit

A further tactic concerned the low pressure steam transport pipe since more steam for the purpose of cooling could be obtained by taking the steam, originally used to generate power, from between the turbine stages. This replaced the diversion of the bleed steam for feedwater heater 3. Figure 17 shows the LP turbine was divided into two LP units in series. Some steam (stream s40) passed directly from the first to the second LP turbine but some (stream s26 followed by s38) was diverted to the cooling jacket. The wall temperature of the transport pipe was controlled to the set point of 600 °C by diverting only a fraction of the exhaust from turbine LP1. The surface temperatures are shown in Figure 18 (a). In principle, the limit was achieved with $w = 2.5$ mm; however the corresponding notional pressure losses in the cooling jacket were sometimes unphysically high. To indicate notional pressure losses, in Figure 18b, the major

losses in cooling jackets, Δp , were estimated from the classical Darcy-Weisbach equation [35],

$$\Delta p = \frac{1}{2} f_d \rho \frac{L}{D_{hyd}} \left(\frac{4\dot{m}}{\pi \rho D_{hyd}^2}\right)^2 \tag{12}$$

where $D_{hyd} = 0.2\,\text{m}$ is the assumed hydraulic diameter of the annular cooling duct, f_d is the Darcy friction factor, and the bracketed terms yield the average steam velocity. The estimated pressure loss was decoupled from the thermodynamic calculation of cycle efficiency. The smallest pressure loss was 3.8 bar for a coating thickness of 5 mm, compared with a working steam pressure, $p_{26} = p_{40}$, of 6.2 bar so that the return coolant (at $p_{38} = 6.2 - 3.8 = 2.4\,\text{bar}$) could not be fed directly to the next turbine stage. This steam could be used in a parallel turbine where the lower inlet pressure would be detrimental to cycle efficiency.

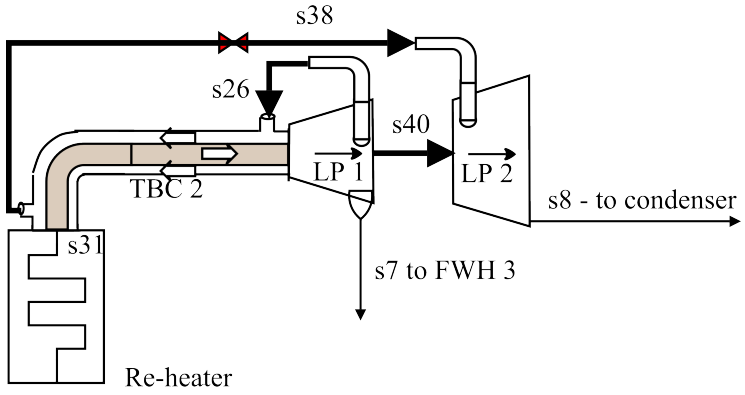

Figure 17: Alternative source of coolant steam for the low pressure transport pipe (TBC 2)

The pressure loss could be mitigated with a larger hydraulic diameter for the cooling duct. From equation (12) the pressure loss, Δp, is approximately proportional to D_{hyd}^{-5}, so a doubling of the hydraulic diameter reduce pressure loss by a factor of roughly 32. A greater hydraulic diameter would be to the disadvantage of capital costs and heat transfer, and would require detailed optimisation by designers. Ignoring pressure losses, and for the thickest layer ($w = 5$ mm) the cycle efficiency was, superficially, 0.3% greater than the baseline case (that is 51.7% vs 51.4%).

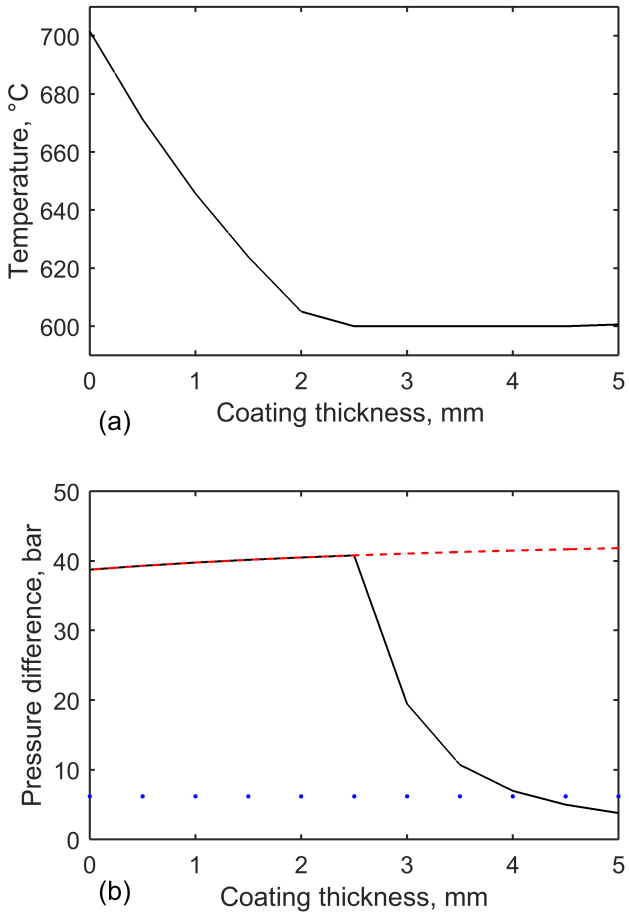

Figure 18: Notional pressure loss across the cooling jacket of TBC pipe 2, according to the Darcy-Weisbach equation, Equation 12 (a) Maximum pipe temperature, with attempt to control at 600 °C (b) notional pressure difference across the cooling jacket (major losses): ——— controlled flow of coolant ; - - - - - - maximum flow of coolant ($\dot{m}_{40} = 0$); . . . . . working steam pressure

.

4.4. Pressure Losses in the Coolant Steam

Figures 19 (a) to (c) consider the impact of frictional pressure losses in the coolant flow in both pipes. In the baseline case, the assumed pressure losses were 5 bar in the higher pressure transport pipe (TBC 1) and zero pressure loss in the lower pressure transport pipe (TBC 2). The impact of pressure losses in TBC pipes 1 and 2 on cycle efficiency are shown in Figure 19(a) and Figure 19(b). As one would expect, the reductions in pressure at the turbine inlets resulted in less power output [16].

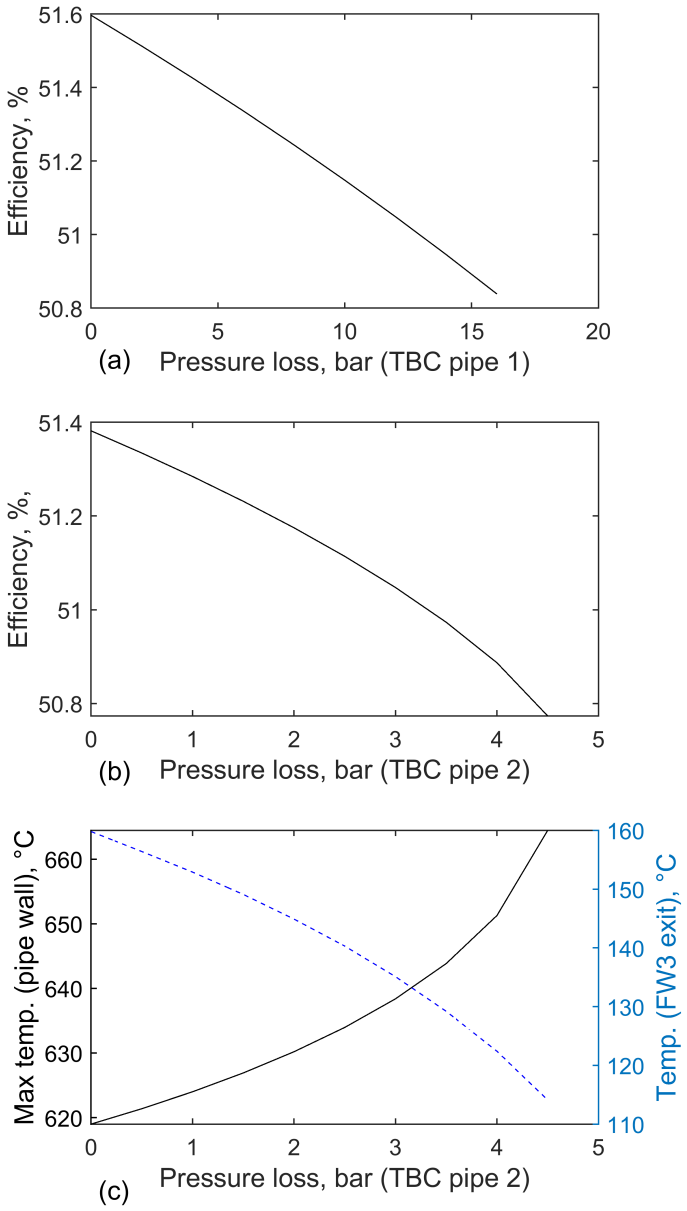

Figure 19: Effect of pressure losses across cooling jackets (a) cycle efficiency vs. pressure loss in high pressure transfer pipe (TBC 1) (b) cycle efficiency vs. pressure loss in low pressure transfer pipe (TBC 2) (c) temperatures vs. pressure loss in low pressure pipe (TBC 2): ——— pipe wall temperature, - - - - - - exit temperature of feedwater heater 3.

.

With regard to the lower pressure transport pipe (TBC 2) the use of the same steam in two successive operations - cooling the transport pipe and then heating the feedwater (FW3) - has interrelated impacts on cycle efficiency and

wall temperatures. Lower steam pressures (stream 7) reduce (1) the saturation temperature within the vapour space of Feedwater Heater 3; (2) the corresponding exit feedwater temperature (at stream s11); (3) the amount of heat recovered in Feedwater Heater 3; (4) the mass flow rate of bleed steam, $\dot{m}_7$, necessary to maintain this restricted heat recovery. The reduced $\dot{m}_7$ brings about the higher pipe wall temperatures in the lower pressure pipe (TBC 2).

4.5. Sensitivity Analysis

The key model parameters for the TBC coated pipes are the thermal conductivities and the heat transfer coefficients, especially for the supercritical steam. The key performance parameters are the overall cycle efficiency and the pipe maximum surface temperature. The sensitivity of these performance parameters to the model parameters are given by

$$s_\eta = \phi \frac{d\eta_{cycle}}{d\phi} \tag{13}$$

$$s_1 = \phi \frac{dT_{TBC1,max}}{d\phi} \tag{14}$$

$$s_2 = \phi \frac{dT_{TBC2,max}}{d\phi} \tag{15}$$

where ϕ represents an uncertain parameter - a heat transfer coefficient, α, or a thermal conductivity, λ. For example a 1% incease in the working fluid heat transfer coefficient, α_{wf}, would result in a reduction in cycle efficiency yielding $\delta\eta_{cycle} = -0.015 \times 0.01 = -0.00015\%$. The sensitivities are given in Table 2. The largest uncertainty is in the fluid heat transfer coefficients, but the results reveal the least sensitivity to these parameters and more sensitivity to the thermal conductivities of the pipe and the thermal barrier coating. This offers additional incentive for research into materials, especially the thermal barrier coating because improved TBC materials could further reduce pipe wall temperature or allow thinner coatings to be used.

Table 2: Sensitivity of three indicators to uncertainty in input parameters.

Parameter	Sensitivity		
	Cycle efficiency, %	Maximum temperature, ^oC	
	s_η	$s_1(T_{TBC1})$	$s_2(T_{TBC2})$
Heat transfer coeff (working fluid), α_{wf}	-0.015	2.187	4.642
Heat transfer coeff (coolant), α_{co}	-0.062	-2.798	-5.164
Thermal conductivity (coating)	-0.307	2.946	32.942
Thermal conductivity (steel)	-0.257	-59.177	-16.023

5. Discussion

There is an overall challenge to increase the operating temperature of future electrical power generating plants together with achieving an operating life of about 60 years [3]. In order to meet these demands we have considered

steam pipe requirements and explored the option of a cooled thermal barrier coated steam pipe to reduce the need to use specific high cost materials, such as nickel based alloys, to achieve resistance to the high operating temperatures. We have modelled the effects of using a typical thermal barrier coating such as yttrium stabilised zirconia applied to a steel pipe on the overall performance of the plant.

A summary of the results is shown in Table 3. The additional simulation of the customary plant on row 1 was performed at sub-critical conditions taken from Retzlaff and Rueggers [4] where the throttle pressure of 165 bar, superheat temperature of 538 °C and reheat exit temperature of 538 °C are used for comparison. This gives an overall cycle efficiency of 42.1% for the customary plant with subcritical conditions. The approach demonstrates that there is a large gain in cycle efficiency of 52.2%-42.1%= 10.1% from moving to A-USC conditions (row 2), which is in-line with Marriot *et al.* [1]. Using the TBC cooled steam pipes lowers the efficiency gain, by around 1% to 9% (row 3). The lower efficiency is offset by the reduction in the need for expensive high temperature special steels and nickel based materials, thus lowering the plant capital cost and the required financing.

The cycle efficiency improves with shorter lengths of steam pipe as less heat is lost from the working fluid. This would drive the design of plants with TBC towards shorter steam transfer pipes wherever possible. The modelling has

Table 3: Cases investigated. Parameters (unless otherwise stated) are superheat = 700 °C, reheat = 720 °C, w = 5 mm, L = 200 m, $\Delta p(TBC1)$ = 5 bar, $\Delta p(TBC2)$ = 0 bar, no HARP

Modification	Figure	Cycle efficiency %	Max. surface temp., °C	
			TBC pipe 1	TBC pipe 2
Sub-critical, 165 bar, 538 °C, 538 °C	-	42.1	538	538
Customary (no TBC)	2	52.2	700	720
TBC applied				
Baseline	3	51.4	564	617
Reduce reheat to 700 °C	3	51.2	560	600
Controlled flow in TBC pipe 1	13	51.4	600	617
Co-current cooling	15	51.4	546	605
Divert LP turbine 1 exhaust through TBC 2 jacket	17	51.7	560	601
Reduce applied Δp in TBC 1 jacket to 0 bar	3	51.6	560	617
Increase applied Δp in TBC 2 jacket to 4.5 bar	3	51.1	600	638

demonstrated that the thermal barrier coating system was successful in keeping the surface temperature in the steam pipe from the supercritical boiler below the target temperature of 600 °C with a barrier coating of 2.8 mm. Keeping the surface temperature below 600 °C in the steam pipe after the reheater was more difficult and would require an estimated coating thickness of around 6.7 mm. This was greater than the current maximum thickness tested in open literature of 4 mm [13]. However, some articles discuss the industrial use of even thicker coatings, but omit any peer-reviewed evidence [36]. The present calculations are based on existing ceramic coatings. It is conceivable that advances with ceramic aerogels [37, 38] would substantially improve thermal resistivity so as to allow thinner coatings, providing their structural strength was adequate. Using the current coating, lowering reheat temperature to below 700 °C (row

4) it is possible to keep surface temperature below 600 °C for yttrium stabilised zironia thickness of less than 5 mm. Alternatively, by splitting the low pressure turbine into two (row 7), more coolant was provided by using the exhaust steam from the first low pressure turbine which kept the required coating thickness below 4 mm. However pressure losses in the coolant could then cause problems when it is used for the second LP turbine.

The cooling jackets attached to transport pipes introduced additional pressure losses that further reduced cycle efficiencies. In this work the pressure loss in the coolant was decoupled from the thermodynamic analysis but hypothesised pressure losses reduced cycle efficiency. Due to the lower density of low pressure steam, greater pressure losses are likely in the lower pressure parts of the cycle, such as the coolant channel around the second TBC coated pipe which is at 6 bar in the proposed design. Even lower pressures would be needed for a double reheat cycle and it could well be that (with coolant flowing at very low pressure) thermal barrier coatings could not be considered for a third length of transport pipe exiting a second reheater. The direction of cooling steam had trivial impact on the overall cycle efficiency but co-current cooling had a beneficial effect on the pipe surface temperatures (row 6). The extra pipework required for a co-current design would lead to larger pressure drops in the coolant resulting in larger cycle loss than counter-current cooling.

The impact of thermal stresses in both the steel wall and the TBC will be a concern. It is a current topic of finite element work and materials testing by collaborators at the Universities of Cranfield and Nottingham, UK [39]. The most challenging feature is thermal cycling between off-load and on-load conditions and it is reassuring that coatings survive even larger temperature oscillations in burner tests. For example Vassen et al [40] report between 1500 and 6000 cycles to failure at combustion gas temperatues up to 1200^oC, decreasing to between 10 and 300 cycles at 1360^oC.

A further concern would be ineffective cooling following changes between off-load and on-load conditions, or owing to a loss of coolant. The risks of thermal transients during load changes and start up in ”customary” plant (no TBC) are well known and are part a comprehensive set of considerations for plant control. The risks are dealt with by prescribed schedules of operation to bring the plant to temperature and, in the UK, certification of a “competent person” to oversee plant operation. Such schedules and certification would have to be rewritten for future designs of A-USC plant, taking into account the additional complexities of the cooling jackets and coatings. The risk of a leak is also an issue for “customary” plant and the authors recognise that in future new inspection methods would have to be developed.

The principle advantages of the TBC approach lie in reducing capital cost and mitigating any insecurity in the supply of base metals. With further development, the calculation procedure presented here would offer design teams the flexibility to select from a large set of options. These include the length of pipe run, the type of coating, coating thickness, and the design of cooling jacket. In future generations of power plant, shorter pipe runs might be facilitated by off-site factory construction or the installation of two-pass boilers. The design and the financial assessment of a new plant item comprise a large, complex project that can take several years - for instance the Babcock and Wilcox design of a supercritical steam generator [18]. Within this time-frame, materials scientists may well develop thicker

coatings, thereby reducing losses of heat, cycle efficiency, and associated revenue from electricity (a loss of 1.9 MWe for the baseline condition). One part of the gross capital cost saving would equal the mass of transport pipes - 1740 tonne for the baseline and "customary" studies - multiplied by the price of nickel superalloy. Over the last seven years the prices of 30 to 42 $\$/kg$ [41] have been roughly 20 times that of steel. The future prices of nickel are uncertain and sensitive to its global scarcity; the open literature contains little concerning the long run prices of base metals [42].

We have shown that the change in cycle efficiency is small compared to the efficiency gains from operating at the higher temperature conditions. There is sufficient justification here for researchers to turn attention to other aspects of the problem. This work shows that the TBC coated pipes are most effective with thicker coatings. Further work needs to be done on (1) methods of applying thick thermal barrier coatings to large sections of pipe (2) the stability of the thermal barrier coating under high temperature steam and oxidising conditions (3) investigation of other coating materials that may allow thinner coatings for the same temperature constraints, and (4) for practical use, inspection, monitoring and repair of coating need to be addressed.

Further modelling work can be done to optimise the plant design, such as the selection of pipe diameters, by coupling the effect of the pressure loss in the coolant jackets to the thermodynamic analysis. A finely detailed optimisation of the diameter of the transport pipe would balance pressure loss (reduces with larger diameter) against area available for heat loss (increases with larger diameter, albeit with a reduced heat transfer coefficient). From the modelling work the conditions, temperatures and pressure, can be used to calculate stresses in the pipes which can also be included in the pipe sizing analysis. The designing of the joints between the inner pipe sections and the outer cooling duct will need detailed investigation to minimise pressure losses and avoid hot spots. Additionally dynamic effects would need to be investigated, particularly plant start up, to ensure that the temperatures and stresses remain within limits during the plant operating cycle. Ideally, the next steps should combine modelling with a programme of experimental design and validation.

6. Conclusions

(i) The new concept proposed in this paper considers counter-flow TBC coated tubes that could enable the use of conventional ferritic and austenitic steels in preference to specialised high cost alloys at higher operating temperatures. For conditions typical of an A-USC plant the cooled thermal barrier coatings successfully maintained the wall temperatures below a target of 600 °C, for the pipe after the supercritical boiler (TBC 1), with a coating of 2.5 mm.

(ii) Cooling the transport pipe located after the reheater (TBC 2) was more challenging as there was less available coolant and the coating would require an estimated thickness of 6.7 mm. The required coating thickness could be reduced by lowering the reheat temperature or by reconfiguring the low pressure turbine to provide larger quantities of steam as coolant. Alternatively, specialised steels or nickel-based alloys could be employed in parts of TBC 2 to cope with wall temperatures exceeding the target.

(iii) Cooling the steam pipes resulted in an efficiency loss of 52.2%-51.4%= 0.8% for a 200 m pipe compared to

no cooling(the latter would lead to excessively high pipe wall temperatures). This is far less than the gains of 10% from operating at A-USC conditions. The concept favours shorter pipes which result in less efficiency loss and lower pipe wall temperatures.

(iv) Co-current cooling had minimal impact on cycle efficiency but a small beneficial impact on pipe wall temperature. Adjusting coolant flow to avoid overcooling the pipe wall had minimal beneficial impact on cycle efficiency when pressure losses are ignored. Pressure losses can have a substantial impact on cycle efficiency.

Acknowledgements

The authors acknowledge funding from the Engineering and Physical Sciences Research Council under grant EP/R000859/1. They are also grateful for the support of EDF Energy and helpful discussions with Mr A. Morris of EDF Energy, Profs N. Simms and J. Nicholls of Cranfield University, UK, and Profs A. Becker and Wei Sun of the University of Nottingham, UK.

Data Access

The new MATLAB code developed for this paper and the data used in the figures presented in this paper are available at `https://data-bris.acrc.bris.ac.uk/projects/Thermal_Coatings`.

References

[1] J. Marion, O. Drenik, C. Frappart, F. Kluger, M. Sell, A. Skea, R. Vanstonee, P. Walker, Advanced ultra-supercritical steam power plants, in: Proc IEA Clean Coal Centre Workshop: Advanced Ultrasupercritical Coal-fired Power Plants, 2012, pp. 4–2.

[2] T. Allen, F. Balbaud-Celerier, T. Asayama, M. Pouchon, J. Busby, S. Maloy, J. Park, C. Fazio, Y. Dai, P. Agostini, et al., Status report on structural materials for advanced nuclear systems, Tech. rep., Organisation for Economic Co-Operation and Development (2013).

[3] J. Knott, Structural integrity issues with Gen IV proposals: fast reactors and PBMR, Materials Research Innovations 16 (6) (2012) 377–384.

[4] K. Retzlaff, W. Ruegger, Steam turbines for ultrasupercritical power plants, in: POWER-GEN, Vol. 98, 1996, pp. 9–11.

[5] P. S. Weitzel, Steam generator for advanced ultra supercritical power plants 700^oC to 760^oC, in: ASME 2011 Power Conference collocated with JSME ICOPE 2011, American Society of Mechanical Engineers, 2011, pp. 281–291.

[6] S. Zinkle, G. Was, Materials challenges in nuclear energy, Acta Materialia 61 (3) (2013) 735–758.

[7] R. A. Miller, Thermal barrier coatings for aircraft engines: History and directions, Journal of Thermal Spray Technology 6 (1) (1997) 35–42.

[8] N. P. Padture, M. Gell, E. H. Jordan, Thermal barrier coatings for gas-turbine engine applications, Science 296 (5566) (2002) 280–284.

[9] W. A. Nelson, R. M. Orenstein, TBC experience in land-based gas turbines, Journal of Thermal Spray Technology 6 (2) (1997) 176–180.

[10] R. Novak, A. Matarese, R. Huston, A. Scharman, T. Yonushonis, Development of Thick Thermal Barrier Coatings for Diesel Applications, Materials and Manufacturing Processes 7 (1) (1992) 15–30.

[11] X. Cao, R. Vassen, D. Stoever, Ceramic materials for thermal barrier coatings, Journal of the European Ceramic Society 24 (1) (2004) 1–10.

[12] V. Kumar, B. Kandasubramanian, Processing and design methodologies for advanced and novel thermal barrier coatings for engineering applications, Particuology 27 (2016) 1–28.

[13] A. Jadhav, N. P. Padture, F. Wu, E. H. Jordan, M. Gell, Thick ceramic thermal barrier coatings with high durability deposited using solution-precursor plasma spray, Materials Science and Engineering A 405 (1-2) (2005) 313–320.

[14] R. Harth, W. Jansing, H. Teubner, Experience Gained from the EVA II and KVK Operation, Nuclear Engineering and Design 121 (1990) 173–182.

[15] M. Hishida, K. Kunitomi, I. Ikuo, K. Umenishi, T. Tanaka, H. Shimomura, K. Sanokawa, Thermal performance test of the hot gas ducts of Hendel CoolerI31I, Nuclear Engineering and Design 83 (1984) 91–103.

[16] G. F. Rogers, Y. R. Mayhew, Engineering Thermodynamics Work & Heat Transfer, Longman Group Limited, 1980.

[17] S. Kjær, F. Klauke, R. Vanstone, A. Zeijseink, G. Weissinger, P. Kristensen, J. Meier, R. Blum, K. Wieghardt, The advanced supercritical 700^oC pulverised coal-fired power plant, VGB POWERTECH-INTERNATIONAL EDITION- 82 (2002) 46–49.

[18] P. S. Weitzel, Component test facility (COMTEST) phase 1 engineering for 760C (1400F) advanced ultra-supercritical (A-USC) steam generator development, in: ASME 2015 Power Conference collocated with the ASME 2015 9th International Conference on Energy Sustainability, the ASME 2015 13th International Conference on Fuel Cell Science, Engineering and Technology, and the ASME 2015 Nuclear Forum, American Society of Mechanical Engineers, 2015, pp. V001T10A003–V001T10A003.

[19] P. S. Weitzel, Component test facility (COMTEST) phase 1 engineering for 760C (1400F) advanced ultra-supercritical (A-USC) steam generator development, Final technical report doe-fe0024067, US Department of Energy, Office of Scientific and Technical Information (2016).

[20] J. T. DeMasi-Marcin, D. K. Gupta, Protective coatings in the gas turbine engine, Surface and Coatings Technology 68 (1994) 1–9.

[21] M. Holgrem, Matlab central: Xsteam, thermodynamic properties of water and steam, updated on 1 Aug 2018 1.
URL https://uk.mathworks.com/matlabcentral/fileexchange/9817-x-steam-thermodynamic-properties-of-water-and-steam

[22] W. Wagner, A. Kruse, IAPWS industrial formulation 1997 for the thermodynamic properties of water and steam, in: Properties of Water and Steam/Zustandsgrößen von Wasser und Wasserdampf, Springer, 1998, pp. 7–37.

[23] J. K. Salisbury, Steam turbines and their cycles, Wiley, 1950.

[24] C. Weir, Optimization of heater enthalpy rises in feed-heating trains, Proceedings of the Institution of Mechanical Engineers 174 (1) (1960) 769–796.

[25] C. W. Stott, Marine reheat cycles and systems evaluation, Marine Technology Society Journal 7 (3) (1970) 298–342.

[26] J. Jackson, Fluid flow and convective heat transfer to fluids at supercritical pressure, Nuclear Engineering and Design 264 (2013) 24–40.

[27] C. Wang, H. Li, Evaluation of the heat transfer correlations for supercritical pressure water in vertical tubes, Heat Transfer Engineering 35 (6-8) (2014) 685–692.

[28] K. Yamagata, K. Nishikawa, S. Hasegawa, T. Fujii, S. Yoshida, Forced convective heat transfer to supercritical water flowing in tubes, International journal of heat and mass transfer 15 (12) (1972) 2575–2593.

[29] I. Pioro, S. Mokry, Thermophysical Properties at Critical and Supercritical Conditions, in: Heat Transfer-Theoretical Analysis, Experimental Investigations and Industrial Systems, InTech, 2011, pp. 573–592.

[30] D. Stöver, C. Funke, Directions of the development of thermal barrier coatings in energy applications, Journal of Materials Processing Technology 92 (1999) 195–202.

[31] S. Kamal, C. Grandy, M. Farmer, A. Brunsvold, High strength and heat resistant chromium steels for sodium-cooled fast reactors., Tech. rep., Argonne National Lab., Argonne, IL (US) (2004).

[32] T. M. International, Material data sheet p91/t91, 10/2011. thyssenkrupp materials international, 2011, nr.10, 3 p.
URL http://www.s-k-h.com/media/de/Service/Werkstoffblaetter_englisch/Kesselrohre_ASTM/P91_T91_engl.pdf

[33] D. Savage, J. Myers, The effect of artificial surface roughness on heat and momentum transfer, AIChE Journal 9 (5) (1963) 694–702.

[34] S. E. Haaland, Simple and explicit formulas for the friction factor in turbulent pipe flow, Journal of Fluids Engineering 105 (1) (1983) 89–90.

[35] G. Brown, The history of the Darcy-Weisbach equation for pipe flow resistance, Proc. Environ. Water Resour. Hist. 38.

[36] H. D. Steffens, Z. Babiak, M. Gramlich, Some aspects of thick thermal barrier coating lifetime prolongation, Journal of Thermal Spray Technology 8 (4) (1999) 517–522.

[37] J. L. Gurav, I.-K. Jung, H.-H. Park, E. S. Kang, D. Y. Nadargi, Silica aerogel: synthesis and applications, Journal of Nanomaterials 2010 (2010) 23.

[38] P. C. Thapliyal, K. Singh, Aerogels as promising thermal insulating materials: An overview, Journal of Materials 2014 (Article ID 127049). doi:10.1155/2014/127049.

[39] X. Guo, W. Sun, A. A. Becker, A. Morris, M. Pavier, P. Flewitt, M. Tierney, C. Wales, N. Simms, J. Nicholls, S. Mori, Modelling and optimized design of a novel coated steam dual pipe system for use in power plant, in: 15th International Conference on Engineering Structural Integrity, Cambridge, Institute of Materials, Minerals and Mining, 2019.

[40] R. Vaßen, M. O. Jarligo, T. Steinke, D. E. Mack, D. Stöver, Overview on advanced thermal barrier coatings, Surface and Coatings Technology 205 (4) (2010) 938–942.

[41] MetalMiner, Sourcing and trading intelligence for global metals market - nickel alloy 625 sheet, last accessed 5 June 2019 (2019). URL https://agmetalminer.com/metal-prices/nickel-alloy

[42] N. B. Anh, A. Semenov, Trends of base metals prices, Theoretical Economics Letters 5 (04) (2015) 531.